INSTITUTE OF PHYSICS PUBLISHING NANOTECHNOLOGY
Nanotechnology **17** (2006) 4240–4251 doi:10.1088/0957-4484/17/16/040

Bennett clocking of quantum-dot cellular automata and the limits to binary logic scaling

Craig S Lent, Mo Liu and Yuhui Lu

Department of Electrical Engineering, University of Notre Dame, Notre Dame, IN 46556, USA

Received 5 April 2006, in final form 3 July 2006
Published 7 August 2006
Online at stacks.iop.org/Nano/17/4240

Abstract
We examine power dissipation in different clocking schemes for molecular quantum-dot cellular automata (QCA) circuits. 'Landauer clocking' involves the adiabatic transition of a molecular cell from the null state to an active state carrying data. Cell layout creates devices which allow data in cells to interact and thereby perform useful computation. We perform direct solutions of the equation of motion for the system in contact with the thermal environment and see that Landauer's Principle applies: one must dissipate an energy of at least $k_B T$ per bit only when the information is erased. The ideas of Bennett can be applied to keep copies of the bit information by echoing inputs to outputs, thus embedding any logically irreversible circuit in a logically reversible circuit, at the cost of added circuit complexity. A promising alternative which we term 'Bennett clocking' requires only altering the timing of the clocking signals so that bit information is simply held in place by the clock until a computational block is complete, then erased in the reverse order of computation. This approach results in ultralow power dissipation without additional circuit complexity. These results offer a concrete example in which to consider recent claims regarding the fundamental limits of binary logic scaling.

(Some figures in this article are in colour only in the electronic version)

1. Introduction

As device feature sizes decrease steadily with the shrinking of semiconductor transistor size, power dissipation has become clearly identified as a key limiter of continued CMOS (complementary metal-oxide silicon) scaling. Beyond the particular components of the problem in CMOS (e.g. static power versus dynamic power, drain-induced barrier lowering, etc) lurk fundamental questions of heat dissipation and device operation. Just how small can a computational device be? How much heat must it generate?

The fundamental structural limit of scaling is single-molecule devices, since it appears impossible to structure matter at a smaller length scale. Single-molecule devices might offer additional benefits. For example molecular self-assembly might enable vast numbers of devices to be created which are precisely identical. Fabrication costs might also be lowered. Of course many problems remain to be solved in the synthesis and positioning of molecular devices, and indeed there are few specific candidates for the devices themselves. Moreover, though single-molecule devices would permit remarkable functional densities, unless the power dissipation per device is extraordinarily small, the promise of high functional densities will be thwarted by enormous heat dissipation.

A simple estimate shows the magnitude of the problem: imagine an array of molecular devices with an average device footprint of 1 nm × 1 nm operating at 100 GHz. This corresponds to a density of 10^{14} devices cm^{-2}. If in each device a *single* electron were to drop down a potential of 0.1 V (dissipating 0.1 eV) every clock period, then the total power dissipated would be 160 kW cm^{-2}.

In this context, it is natural to ask if there is a certain minimal amount of energy which *must* be dissipated in order to compute a bit. If CMOS at the end of scaling dissipated an

amount close to the theoretical minimum, then searching for other device strategies would be unwarranted—none could do much better. The connection, at first counterintuitive, between information (computation) and heat has its roots in the very beginnings of statistical mechanics, discussions of Maxwell's demon, and the Second Law of Thermodynamics. The history of the question has been ably reviewed by others [1–3] and a brief summary will suffice here.

Szilard and Brillouin argued that the measurement associated with the READ operation causes an energy dissipation of $k_B T \ln(2)$ per bit [4, 5]. Landauer refuted this notion, showing that there is no necessary minimum energy dissipation associated with reading a bit, but rather with erasing information [6, 7]. He argued that logically reversible functions, in which no information is lost, could be performed with as little dissipation of heat as desired, though at the cost of speed. The ERASE operation, or any logically irreversible function, by contrast, must dissipate at least $k_B T \ln(2)$ per bit, independent of the operation speed. If a copy of the bit that is to be erased is kept, the operation can dissipate an arbitrary small amount of energy.

By 'energy dissipation' we mean the transfer of energy from the system to the environment. This is irreversible because of the thermodynamically large number of degrees of freedom of the environment. Energy dissipation is not the same as energy transfer from one part of a circuit to another. Confusion often results from imprecise language, e.g. 'the amount of energy it takes to compute a bit', which fails to distinguish device-to-device energy transfer from energy dissipation (the distinction *is* observed, for example in [8]).

Bennett extended the Landauer result by showing that in principle any computation could be embedded in a logically reversible operation [9]. The simplest version of this is simply to echo a copy of the inputs to the output. One can accumulate the intermediate results, information that would normally thrown away, and then erase these results by reversing the functions that created them. By using the inverse operations of the forwards computation process, the system could be returned to its original state. Unless the original inputs to the calculation are stored, unavoidable dissipation occurs when they are erased.

The minimum of $k_B T \ln(2)$ can be understood from a simple statistical mechanical consideration. Let W be the number of physical configurations the system can be in. If initially the bit system can be in a 1 or 0 state, then $W = 2$. If the information is erased then for the final state $W = 1$. This 2-to-1 transition results in an entropy change for the system of $\Delta S = k_B \ln(1) - k_B \ln(2) = -k_B \ln(2)$. Since the Second Law of Thermodynamics requires that $\Delta S \geqslant 0$, the environment must increase in entropy by at least $+k_B \ln(2)$. This results in a free energy transfer to the environment of $\Delta F = T\Delta S = k_B T \ln(2)$.

There remains a question of practicality. Is it a practical possibility to do computing in a reversible (or nearly reversible) way? Keyes, a coauthor with Landauer on some of the pioneering papers, assessed the situation in a 2001 article on the 'Fundamental Limits of Silicon Technology'. His statement was terse and gloomy:

> 'Charles Bennett showed in 1973 that computation could be carried out in principle without dissipation of energy with thermodynamically reversible operations, avoiding the discarding of information. However, a practical implementation of reversible computing has not occurred [10]'.

It seems likely that pressing *transistors* into service to implement reversible computing will prove finally not to be a practical approach.

One promising approach to molecular-scale electronics is quantum-dot cellular automata (QCA) [11–65]. In contrast to transistors which function as current switches, QCA employ cells through which no current flows. Binary information is encoded in the charge configuration of the cell. A local electric field provides a clocking signal which controls the activity of the cell and can smoothly switch it from an information-bearing 'active' state to a non-information-bearing 'null' state. Prototype QCA circuits have been fabricated using metal tunnel junctions in the single-electron regime [24–32] and considerable progress has been made towards implementing molecular QCA [33–43]. The QCA clocking scheme that has been developed relies on switching the cell to an active state adiabatically, that is, gently enough that it is always very close to its instantaneous ground state, applying the ideas of Landauer [34, 38]. This approach reduces power dissipation to its essentials, dissipating significant amounts only when information is erased [22, 23].

Other aspects of QCA operation need be mentioned only briefly here:

- *Power gain* in QCA has been demonstrated theoretically [22], and experimentally [31]. The clock provides energy to make up for that lost due to dissipative processes.
- *Defect tolerance* is crucial for any molecular-scale technology because defects in layout are unavoidable. The QCA approach is inherently robust and can be made even more so by simply using wide (3- or 5-cell) wires to build in redundancy at every stage. Other defect-tolerant strategies in QCA are under investigation [44–46].
- *New architectures* must be created to match new transistorless computational paradigms. Significant work on this front has been done [47–59], though much more remains to be explored. The development of QCA design tools such as *QCADesigner* [60] is particularly helpful in this regard.
- *Other realizations* of QCA which have been demonstrated include silicon quantum dots [61, 62], and magnetic domains [63–65].

We focus here on clocked molecular QCA, where the clock signal is a time-varying perpendicular electric field as described above. We note that the QCA approach is one of several alternatives to harnessing the unique features of quantum dots to implement logical computation [66–74].

In this paper we explore the application of the ideas of Bennett to switching QCA devices in the most power-efficient manner possible, preserving intermediate results *in place* so that power dissipation is reduced even further. The efficacy of the Landauer–Bennett approach is made clear by directly solving the equations of motion for irreversible, reversible, and Bennett-clocked gates. We show that QCA provide a natural implementation of Bennett switching which could offer both

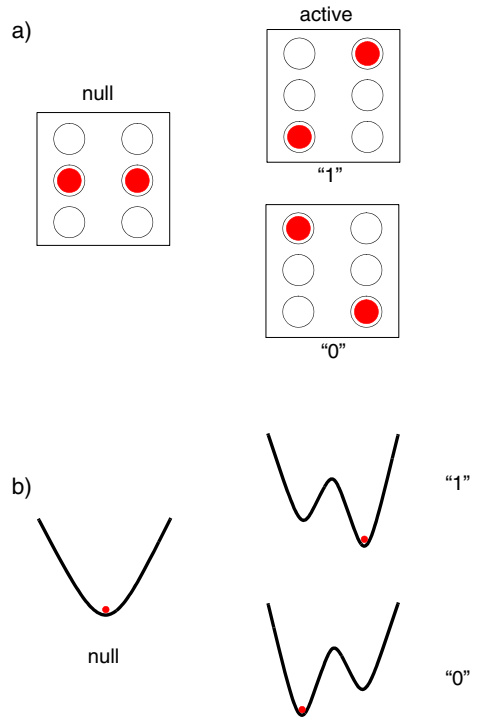

Figure 1. (a) Schematic diagram of a QCA cell. The cell is comprised of dots, which are sites that localize charge. The configuration of charge is used to represent a 1 or 0 bit, or a null state which carries no information. Not shown is the fixed neutralizing charge which maintains the cell's overall charge neutrality. A clocking signal shifts the relative energies the null state and the active (1 or 0) states. (b) Schematic potential energy diagram for the null state and the two active states. The clock changes the system from a monostable (null) to a bistable (active) configuration. The presence of neighbouring cells breaks the degeneracy between the 1 and 0 state.

a practical realization of reversible computing and one that could be scaled to the limit of single-molecule devices. In the last section we discuss the implications of our results for the broader question of the ultimate limits of binary-switched computing. We contrast our results with the arguments of Zhirnov *et al* [75, 76].

2. Quantum-dot cellular automata

A schematic clocked QCA cell is shown in figure 1(a). Two mobile electrons are confined to the cell. Within the cell the electrons are distributed among six dots. Dots are simply regions in which charge is localized. Three possible charge configurations are shown in the figure, the electrons in corner dots representing either a binary '1' or '0', and electrons both in the middle dots representing a 'null' state which contains no binary information. Tunnelling between the dots enables the state of the cell to switch.

In normal operation the QCA cell will be in, or very close to, its ground-state configuration throughout a switching event. Which of the possible cell charge configurations is the ground state is determined by two factors: (1) the electronic configuration of the neighbouring cells, communicated to the cell through the Coulomb interaction which alters the potential on each dot, and (2) a *clocking field* which alters the relative energy of occupying the middle 'null' dots versus the corner 'active' dots. If the clock pulls the electrons into the null dots, then the cell is forced into the null state regardless of the state of the neighbours. If the clock pushes the electrons out of the null dots into the active dots, then the cell will be put into whichever active state has the lowest energy. The low-energy active state will be determined by the configuration of the neighbouring cells.

When the clocking field is sufficiently strong, it can also 'latch' the state of the cell. The QCA cell is designed so that to switch from one active configuration to the opposite configuration the cell must go through the null configuration, i.e. it must switch though the path [0 → null → 1] or [1 → null → 0]. This is why the null dots are in the middle. As a result, if the clock raises the occupation energy of the null sufficiently high, it creates a kinetic barrier to switching which latches (locks) the state of the cell. A latched cell acts as a single-bit memory—its present state depends on its state in the recent past and *not* on the state of neighbours. A latched cell is not necessarily in its instantaneous ground state.

QCA represent a specific implementation of Landauer's notion that computing can be accomplished, with minimal power dissipation, by using elements that switch from a monostable to bistable state in a controlled and adiabatic way. Figure 1(b) shows a schematic energy level diagram for the cell. In the null state, the cell is monostable. When the potential energy of the middle dots is raised, creating a barrier between the two active states, the cell becomes bistable. If there were no other influence on the cell the two local minima would have the same energy. The presence of nearby cells lowers the energy of the well corresponding to either the '1' or '0' state.

We can see how information is moved from cell to cell by considering the simple case of the COPY operation between two adjacent cells, illustrated in figure 2. Suppose the cell on the left is in the active 1 state and the cell to its right is initially in the null state. The clock for the cell to the right is then raised. This causes the right cell to switch into the 1 state as well—the field from the left cell raises the energetic cost of being in the 0 state relative to the 1 state. This transition can be accomplished gradually so that the rightmost cell is always very close to its instantaneous ground state and thus can dissipate very little energy. The time scale for 'gradually' is set by the tunnelling time from one dot to the next. A QCA shift register can be constructed by copying a bit from cell to cell in a linear cell chain, shown schematically in figure 3(a).

Information can not only be moved, but processed. A three-input majority gate is formed when three QCA shift registers converge as shown in figure 3(b). The additive effect of the Coulomb interaction from the input cells determines which state the device cell (at the junction) will switch into when its clock is raised. The result is then transported (to the right in this case) down the output shift register. A complete set of functions can be realized and more complex circuits constructed hierarchically [15, 18].

QCA devices exist. Functional QCA cells have been fabricated using aluminium islands on SiO_2 to form the dots, which are coupled through aluminium oxide tunnel junctions and patterned capacitors [24]. QCA devices have

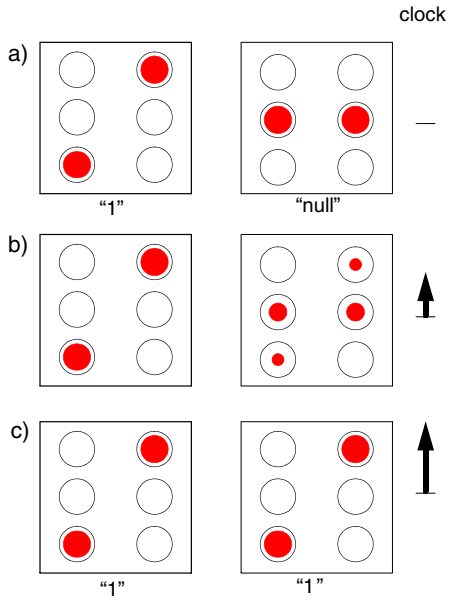

Figure 2. The copy operation between two QCA cells. (a) The cell on the left holds the 1 bit and the adjacent cell is initially null. As the clock on the right cell is raised, (b) → (c), the information is copied into the right cell. Physically, this occurs because the potential on the middle dots is raised, and the charge moves off into the corner dots. The lower energy configuration is that matching the configuration of the cell on the left. The non-integer average occupancy in (b) is due to either quantum uncertainty or thermal fluctuations, or both.

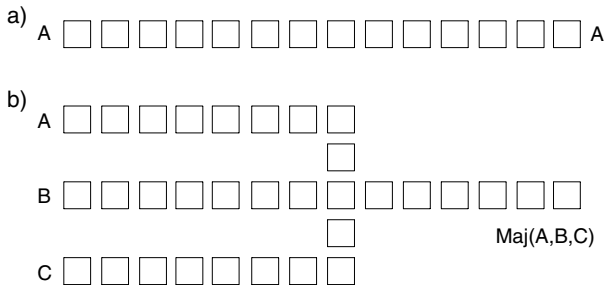

Figure 3. Schematic layout of QCA cells forming devices. (a) A shift register in which information is simply copied from cell to cell down the line. (b) Three shift registers converge at a single cell to form a three-input majority gate.

so far been constructed from tunnel junctions fabricated with shadow-evaporation techniques and function only at cryogenic temperatures. A number of circuits including majority gates and clocked shift registers have been demonstrated [25–32]. In these metal-dot QCA cells it is straightforward to separately clock each cell individually using capacitively coupled voltage leads. It is noteworthy that, in these devices, information is represented by the configuration of two electrons per cell. Thus these metal-dot cells, though limited by the fabrication method to low-temperature operation, provide valuable demonstrations of QCA circuits. They serve as prototypes for molecular systems that will function at room temperature.

Significant steps have been taken towards constructing single-molecule QCA cells using mixed valence compounds. One key strategy is to use non-bonding π or d orbitals to serve

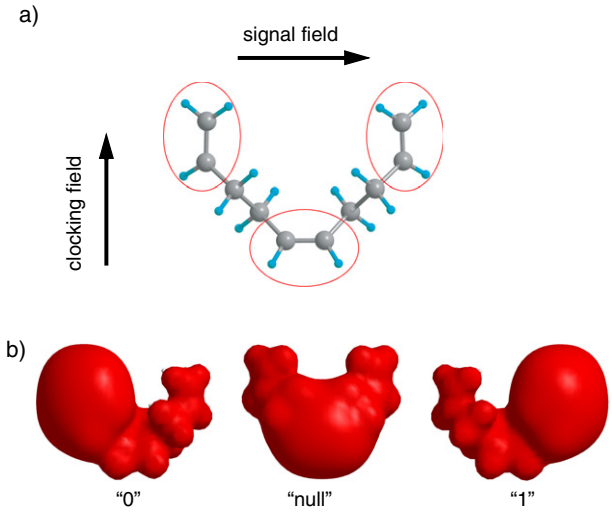

Figure 4. A molecular QCA half-cell. (a) The model molecule has three dots formed from ethylene groups. The molecular cation has a mobile hole which can occupy one of the three dots, representing a binary 1 or 0 and the null state. (b) Isopotential surfaces show the localization of charge in the three states. A transverse electric field carries the signal from the neighbouring molecules. A perpendicular electric field acts as a clock which moves the state between active (1 or 0) and null. This molecule lacks any functionalization for attachment and orientation, but is useful as a model system made computationally tractable by its simplicity. Synthesized candidate QCA molecules are described in [40–43].

as dots, so that electron transfer from dot to dot has minimal effect on the overall molecular structure [33–43]. Two-dot half-cells [40–42] and four-dot cells [43] have recently been synthesized. The two-dot cells were functionalized for attachment to a silicon substrate by covalent bonding. Supporting groups act as 'struts' which hold the molecule perpendicular to the surface. Direct measurements of the bistable switching required for QCA operation have been reported [42]. Charge tunnelling from one dot to the other is sensed by capacitance measurements.

Quantum chemistry calculations [77] of simple molecules with QCA properties can be useful in understanding molecular QCA switching behaviour. Figure 4(a) shows a simple three-dot clocked half-cell composed of only carbon and hydrogen. The molecule lacks any functionalization for attachment and orientation, but is useful as a model system and is made computationally tractable by its simplicity. Ethylene groups form the dots in this structure. The molecular cation has a mobile hole which can occupy one of the three dots. Isopotential surfaces plotted in figure 4(b) show the molecular cation in the three states corresponding to 0, 1, and null. An electric field in the z-direction acts as a clocking field and the field in the y-direction, presumably due to neighbouring molecules, is the input signal. The information content of the molecule is represented by the y-component of the dipole moment. We define the polarization to be the normalized dipole moment

$$P = \frac{\mu_y}{|\mu_y(\mathrm{max})|}. \tag{1}$$

Figure 5 shows the calculated polarization as a function of the clocking field in the presence of a signal (driver) field of either

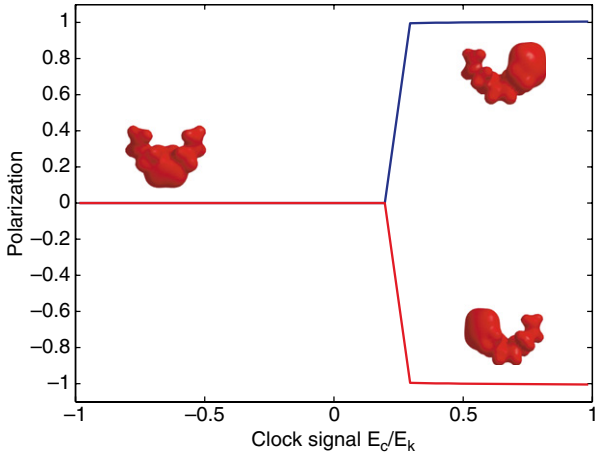

Figure 5. Calculated response for molecular QCA. The response of the molecule shown in figure 4 to a clock signal in the presence of a signal field. The clocking field shifts the relative potential energies of the upper dots and the lower dots by an amount E_c. The horizontal axis is the ratio of this energy shift to the 'kink energy' E_k which represents the interaction between two molecules. The cell polarization is the normalized molecular dipole moment. The two curves are for signal fields of opposite signs. The clock causes the molecule to move from the null state to the appropriate polarized cell.

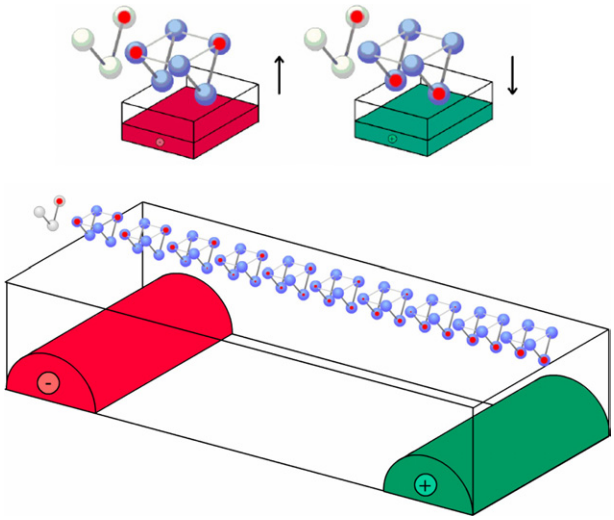

Figure 6. Clocking in a molecular QCA cell array. Buried conductors form clocking wires which produce the clocking field at the molecular layer. By driving adjacent wires with phase-shifted sinusoidal voltages, the active regions in the molecular layer shift smoothly across the surface.

sign. The clocking field activates the cell, pushing it into the appropriate state depending on the sign of the driver field.

Molecular QCA devices can be clocked without having to make separate clock connections to individual molecules [34, 35, 38]. Buried clocking wires can be used to form a patterned time-varying inhomogeneous perpendicular electric field (E_z) at the molecular QCA plane which acts as a clocking signal. Shifted sinusoidal clocking phases applied to successive wires result in a continuously varying distributed clock signal that smoothly sweeps information along the QCA shift register. Figure 6 illustrates this process schematically. In this case adjacent molecules see clocking signals that are only fractionally out of phase with one another. This makes the adiabatic transition all the more smooth, but still directs the propagation down the circuit towards the output. This approach avoids the need to make separate contacts to individual molecules, which would be impractical.

3. Modelling QCA dynamics with dissipation

We can describe the relevant physics of QCA switching in a thermal environment using a simplified three-state basis and a version of the coherence-vector formalism [78]. The three basis states correspond to the 1, 0, and null states of the cell (molecule). A Hamiltonian is constructed that includes (a) the effect of the input signal which shifts the relative energies of the 0 and 1 states, (b) the effect of the clocking field which shifts the energies of the active states relative to the null state, and (c) tunnelling between the states. The Hamiltonian for the jth cell at time t is given by

$$H^{(j)}(t) = \begin{bmatrix} -\frac{E_k}{2}\sum_{m\neq j} f_{j,m}P_m(t) & 0 & -\gamma \\ 0 & +\frac{E_k}{2}\sum_{m\neq j} f_{j,m}P_m(t) & -\gamma \\ -\gamma & -\gamma & E_c(t) \end{bmatrix} \quad (2)$$

where E_k is the 'kink energy', the energy difference between two horizontally adjacent polarized cells having the same polarization or the opposite polarization. It can be calculated from simple electrostatics. γ is the tunnelling energy between the active states and the null state. This can be obtained for a particular molecule from quantum-chemistry calculations. P_m is the polarization of the mth cell. $f_{j,m}$ is a geometric factor depending on the distance and relative orientation between the jth cell and the mth cell. It is computed from electrostatics. E_c is the potential energy of the null state which is altered by the clock. The zero of energy is here chosen to be that of an active isolated cell.

Following [78] we employ the eight generators of the Lie group $SU(3)$,

$$\hat{\lambda}_1 = \begin{bmatrix} 0 & 1 & 0 \\ 1 & 0 & 0 \\ 0 & 0 & 0 \end{bmatrix} \quad \hat{\lambda}_2 = \begin{bmatrix} 0 & 0 & 1 \\ 0 & 0 & 0 \\ 1 & 0 & 0 \end{bmatrix}$$

$$\hat{\lambda}_3 = \begin{bmatrix} 0 & 0 & 0 \\ 0 & 0 & 1 \\ 0 & 1 & 0 \end{bmatrix} \quad \hat{\lambda}_4 = \begin{bmatrix} 0 & \mathrm{i} & 0 \\ -\mathrm{i} & 0 & 0 \\ 0 & 0 & 0 \end{bmatrix}$$

$$\hat{\lambda}_5 = \begin{bmatrix} 0 & 0 & \mathrm{i} \\ 0 & 0 & 0 \\ -\mathrm{i} & 0 & 0 \end{bmatrix} \quad \hat{\lambda}_6 = \begin{bmatrix} 0 & 0 & 0 \\ 0 & 0 & \mathrm{i} \\ 0 & -\mathrm{i} & 0 \end{bmatrix} \quad (3)$$

$$\hat{\lambda}_7 = \begin{bmatrix} -1 & 0 & 0 \\ 0 & 1 & 0 \\ 0 & 0 & 0 \end{bmatrix} \quad \hat{\lambda}_8 = \frac{1}{\sqrt{3}}\begin{bmatrix} -1 & 0 & 0 \\ 0 & -1 & 0 \\ 0 & 0 & 2 \end{bmatrix}$$

to project out the real degrees of freedom of the density matrix for the jth cell $\hat{\rho}_j$.

$$\lambda_k^{(j)} = \mathrm{Tr}(\hat{\rho}_j\hat{\lambda}_k). \quad (4)$$

These generators, $\hat{\lambda}_k$, play the same role for $SU(3)$ that the Pauli spin matrices play for $SU(2)$. The state of each cell j is then described by the eight-dimensional vector, $\vec{\lambda}^{(j)}$. The cell

polarization can then be defined in terms of the expectation value of a particular generator.

$$P_j = -\mathrm{Tr}(\hat{\rho}_j \hat{\lambda}_7) = -\lambda_7^{(j)}. \tag{5}$$

The Hamiltonian determines the eight-dimensional real vector with components

$$\Gamma_{\mathrm{k}}^{(j)} = \mathrm{Tr}(\hat{H}^{(j)} \hat{\lambda}_{\mathrm{k}}), \tag{6}$$

and the 8×8 matrix

$$\Omega_{mn}^{(j)} = \sum_p f_{mpn} \Gamma_p^{(j)} \tag{7}$$

where f_{mpn} are the structure constants for $SU(3)$ defined by the relation

$$4\mathrm{i} f_{mpn} = \mathrm{Tr}\{[\hat{\lambda}_m, \hat{\lambda}_p] - \hat{\lambda}_n\}. \tag{8}$$

In isolation from the environment the unitary evolution of the density matrix can be expressed as the equation of motion for the coherence vector.

$$\frac{\partial}{\partial t} \vec{\lambda}^{(j)}(t) = \Omega^{(j)}(t) \vec{\lambda}^{(j)}(t). \tag{9}$$

Equation (9) represents a set of coupled first-order differential equations for the motion of the coherence vectors of each of the cells. If each cell were in a pure state, it would be equivalent to the Schrödinger equation. For mixed states (9) is equivalent to the quantum Liouville equation. The Coulomb interaction between the cells is included in a mean-field Hartree approximation through (2).

The description can now be enlarged to include contact with a thermal environment and dissipation (following [22] and [23]). The density matrix for the jth cell in thermal equilibrium with its environment at temperature T is

$$\hat{\rho}_{\mathrm{th}}(t) = \frac{\mathrm{e}^{-\hat{H}^{(j)}(t)/k_{\mathrm{B}}T}}{\mathrm{Tr}\{\mathrm{e}^{-\hat{H}^{(j)}(t)/k_{\mathrm{B}}T}\}}. \tag{10}$$

The associated equilibrium coherence vector is

$$[\vec{\lambda}_{\mathrm{th}}^{(j)}(t)]_{\mathrm{k}} = \mathrm{Tr}\{\hat{\rho}_{ss}(t) \hat{\lambda}_{\mathrm{k}}\}. \tag{11}$$

Dissipation can be expressed using an energy relaxation time approximation. The non-equilibrium equation of motion for the jth cell in contact with the thermal environment is then

$$\frac{\partial}{\partial t} \vec{\lambda}^{(j)}(t) = \Omega^{(j)}(t) \vec{\lambda}^{(j)}(t) - \frac{1}{\tau}[\vec{\lambda}^{(j)}(t) - \vec{\lambda}_{\mathrm{th}}(t)]. \tag{12}$$

The coherence vector is driven by the Hamiltonian forcing terms, and relaxes to the instantaneous thermal equilibrium value. The energy relaxation time τ characterizes the dissipative coupling between the system and the environment. Because for QCA the quantum phase difference between cells is irrelevant, we need not include a separate phase relaxation time (using QCA for quantum computing has been explored in [21]).

The non-equilibrium equation of motion (12) represents a set of coupled first-order differential equations for the coherence vectors of QCA cells in contact with the thermal environment. As above the cell-to-cell coupling is treated in a mean-field approach ([20] extends this treatment beyond the mean field). Coupling with the environment allows thermal fluctuations to excite the cells, and for cells to dissipate energy irreversibly to the environment. All the essential elements to study the thermodynamics of computation in an open quantum system are present in this description.

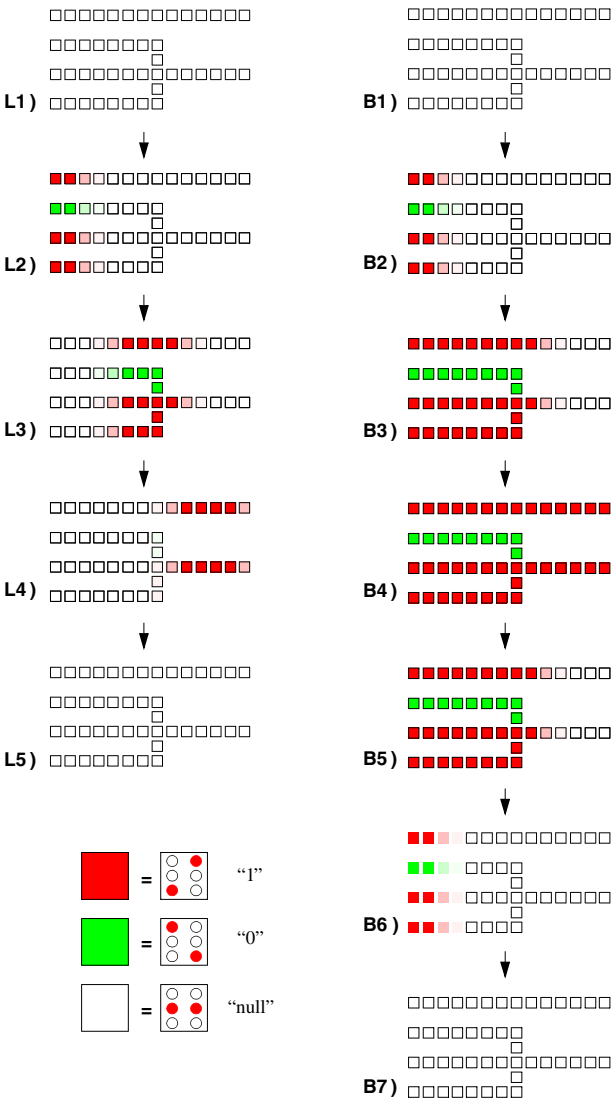

Figure 7. Landauer and Bennett clocking of QCA circuits. Each figure represents a snapshot in time as the clocking fields move information across the circuit. The left column (L1)–(L5) represents Landauer clocking. A wave of activity sweeps across the circuit as the clocking field causes different cells to switch from null to active. The circuit shown includes a shift register on top and a three-input majority gate on the bottom. The right column (B1)–(B7) represents Bennett clocking for a computational block. Here as the computational edge moves across the circuit intermediate results are held in place. When the computation is complete (B4), the activity sweeps backwards, undoing the effect of the computation. This approach yield the minimum energy dissipation.

4. Landauer and Bennett clocking of QCA

Figure 7 illustrates Landauer and Bennett clocking of QCA circuits. The figure shows a QCA shift register, implemented by a single line of cells, and a three-input majority gate. The left column (L1–L5) represents snapshots of the circuit at different times as it is clocked using the Landauer clocking scheme and the right column (B1–B7) shows snapshots using the Bennett clocking scheme. It is assumed that the input signals come from other QCA circuitry to the left of the circuit shown and that the output signals are transported to the right to other QCA circuits.

The motion of the information across the array is not ballistic, but controlled by the clocking signals. These clocking signals could be implemented in several ways, but for specificity here let us focus on molecular QCA controlled by a swept perpendicular electric field produced by local clocking wires as shown in figure 6. The effect of the clocking field is to gradually drive cells in a particular region from null to active and back to null. Whether the active state is a 0 or 1 is determined by the state of the neighbours.

The Landauer-clocked circuit initially has all cells in the null state (L1). As the clocking signal activates the leftmost cells, they copy the incoming information and propagate it to the right (L2). The shift register (the linear array on the top of each snapshot) simply moves the information from left to right. In the example shown a 1 bit, represented by a group of polarized cells (red = '1'), is transported. The bit moves as cells are activated and copy the bit on the leading edge of the bit packet; cells on the trailing edge are erased to null. Because this trailing-edge cell erasure is done in the presence of a copy of the information (i.e. no information is being lost), it can be accomplished without dissipating $k_B T \ln(2)$. More precisely, there is no fundamental lower limit to the energy that must be dissipated.

In the Landauer-clocked majority gate, shown on the lower part of each snapshot, three bits of data (here a 0, 1, and 1) 'collide' to compute the majority function. The computation happens as the leading edge of the bit packets converge at the central device cell (L2 → L3). Erasure of cells on the trailing edge is comparable to the case of the shift register except for the 'loser' in the majority vote. In that case, because the output cells are in the majority state, an input line must be erased to null without a copy being present. In figure 7, the 0 input to the majority gate loses the vote and the information moving forwards to the right (L4 and subsequent) contains no record that the 0 was ever present. In this case information is really lost to the whole system and an energy of least $k_B T \ln(2)$ must be dissipated as heat (as we will see in the next section).

The speed at which the computation occurs can influence the total power dissipated in a way unrelated to the issue of information loss. In the Landauer-clocked circuit (figure 7(L1)–(L5)) we see a wave of computational activity sweep across the circuit. The leading edge of the wave is where computation actually occurs; the trailing edge is where erasure occurs. The speed of the wave is determined by the clocking frequency and the pitch of the clocking wires. The practical upper limit of clock frequency is determined by one of two requirements: adiabatic operation or power dissipation. If the clock frequency is too fast, cells on the leading edge do not have enough time to switch smoothly to their new state and either oscillate or become stuck in metastable states. 'Too fast' is relative to the tunnelling time for an electron to move from one side of the molecule to the other. This can be very fast indeed; sub-picosecond times have been reported even for large molecules [79]. The gradual adiabatic nature of the switching is also a function of the width of the bit packet set by the clocking wire pitch. A broad gentle edge improves adiabaticity, at the cost of total information density in the pipeline. As the frequency approaches adiabatic breakdown, even for reversible computation like the shift register, cells on the leading edge begin to be excited above their instantaneous ground state. This excess energy in the cell is dissipated as heat as the cells de-excite through inelastic processes (e.g. molecular vibrational states). For a large array of cells at molecular densities, this power dissipation can become the practical limitation, though THz operation of densities as high as 10^{12} devices cm^{-2} may still be a possibility [22]. This heat dissipation due to operating at speeds near adiabatic breakdown is a separate issue from the heat dissipation due to information erasure—the requirement of dissipating at least $k_B T \ln(2)$ per erased bit holds no matter how slow the clock speed.

Bennett-clocked operation is shown in figures 7(B1)–(B7), which again represents snapshots in time as the array is clocked. The computational leading edge of the clocking wave moves from left to right in (B2)–(B4). The difference in the Bennett-clocked circuit is that there is no trailing edge—cells remain held in the active state as the computational edge moves forwards. The loser in the majority gate (the green = '0' input) is held in place and not erased until the results of the computation are present at the (here rightmost) output edge. At that time, the output states can be copied to the next stage of computation and the clock begins to lower cells back to the null state from right to left (B4)–(B7). In this part of the cycle, erasure of intermediate results does occur but always in the presence of a copy. Thus no minimum amount of energy ($k_B T \ln(2)$) need be dissipated. At the end of the back-cycle the inputs to the computation must either be erased or copied. If they are erased, then an energy of at least $k_B T \ln(2)$ must be dissipated as heat for each input bit. This is unavoidable. What *has* been avoided is the energetic cost of erasing each of the intermediate results. The example shown in the figure is only one shift register and one majority gate—in practical cases it would be a large subsection of the calculation. In that case there are many more intermediate results than input bits so the savings in energy dissipation by Bennett clocking could be large.

The Bennett-clocking scheme has benefits and costs which are part of the design space for the circuit. The principal benefit is lower power dissipation, which as we have seen may make the difference between molecular-scale electronics working or vaporizing. The costs include at least doubling the effective clock period to allow the forward and reverse cycles (B1)–(B4) and (B4)–(B7). In addition, the amount of pipelining is reduced because for a given block of computation only one computational edge at a time can be moving across the circuit in the Bennett-clocked scheme. In Landauer clocking, by contrast, several computational waves can be traversing the same block at the same time. Finally, the circuitry that provides the clocking signal has to be somewhat more complex to handle the block-by-block forwards-then-backwards clocking of the Bennett approach. In many circumstances, the speed and simplicity of Landauer clocking will outweigh the power dissipation benefits of Bennett clocking. It is notable that the QCA layout itself does not have to be changed to go from one to another—only the timing of the clocking needs to be altered. One could imagine switching from one mode to the other as needed.

5. Direct comparison of Landauer and Bennett clocking

We employ the formalism described in section 3 above to example circuits with both Landauer and Bennett clocking to

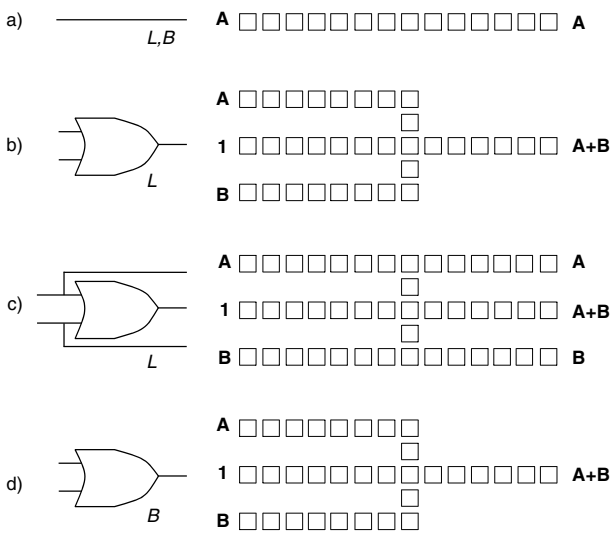

Figure 8. Four test QCA circuits. (a) A shift register, which can be Landauer-clocked or Bennett-clocked. (b) A Landauer-clocked OR gate. (c) A Landauer-clocked OR gate for which inputs are also echoed to the output, embedding a logically irreversible operation in a logically reversible operation. (d) A Bennett-clocked OR gate.

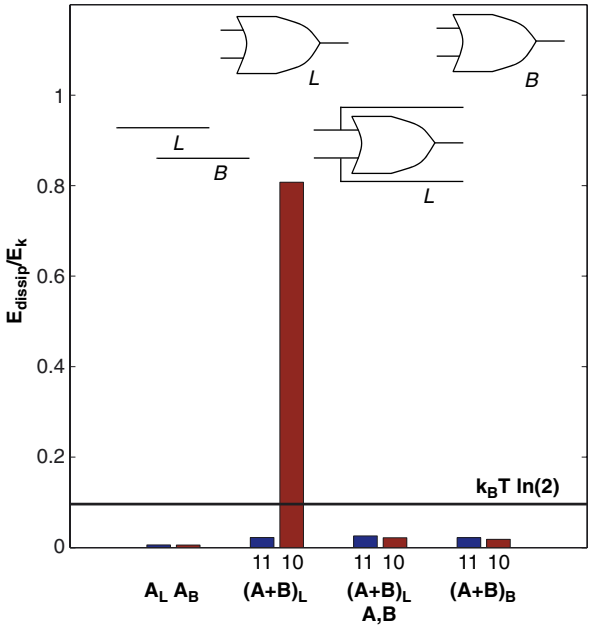

Figure 9. Calculated energy dissipation for the four test QCA circuits in figure 8. The shift registers involve no information loss so dissipate less than $k_B T \ln(2)$. The Landauer-clocked OR gate dissipates much more than $k_B T \ln(2)$ when the input bits differ. Echoing inputs to the output succeeds in reducing energy dissipation, but at the cost of circuit complexity. Bennett-clocking yields very low energy dissipation with no additional circuit complexity.

directly compare the power dissipation in the two approaches. We directly solve equation (12) for each cell in the circuit. Note that $\Omega^{(j)}$ in (12) is derived from the Hamiltonian, equation (2), which depends on the polarization of all of the other cells. (The influence drops as the inverse fifth power of the distance because each cell is an electric quadrupole—so the neighbouring cells dominate the sum in (2).) Equation (12) thus represents a set of $8N_{\rm cells}$ ($\vec{\lambda}^{(j)}$ is an eight-dimensional vector) coupled differential equations which we solve simultaneously for the dynamics of the entire circuit. This captures both the quantum nature of the motion and its contact with the thermal environment.

The form of the clocking wave enters through $E_{\rm c}(t)$ in equation (2). Though the clocking field can be calculated explicitly from the voltage on the clocking electrodes (as in [34]), we here use a simplified description. Landauer clocking is described by

$$E_{\rm c}(t) = E_{\rm C}^0 \sin\left(\frac{x}{\lambda_{\rm c}} - \frac{t}{T_{\rm c}}\right) \tag{13}$$

where $\lambda_{\rm c}$ is the spatial clocking wavelength and $T_{\rm c}$ is the temporal clocking period. Bennett clocking is described by

$$E_{\rm c}(t) = E_{\rm C}^0 \min\left[\left(1 - \frac{x}{\lambda_{\rm c}}\right) + \sin\left(\frac{t}{T_{\rm c}}\right), 1\right] \tag{14}$$

where $\lambda_{\rm c}$ is now the width of the Bennett-clocked region. This represents a linear ramp which sweeps across the region and then back. Bennet-clocked regions can adjoin each other so that the output of one becomes the input to the next; pipelining is altered but preserved.

Figure 8 shows four QCA circuits. The first, shown in figure 8(a), is simply a QCA shift register, which can be Landauer-clocked or Bennett-clocked. A two-input OR gate is formed from a three-input majority gate by fixing one input to a binary 1. Figures 8(b) and (d) represent OR gates with Landauer and Bennett clocking respectively (the actual layout is identical). Figure 8(c) shows an OR gate with the addition of lines echoing the input to the output. This is the usual method of achieving Bennett-style reversible circuitry. It has the drawback that the circuitry is more complex and intermediate results accumulate as the computation proceeds. The QCA circuit represented in figure 8(c) is Landauer-clocked.

Figure 9 shows the energy dissipated per clock cycle for each of the four circuits shown in figure 8, calculated using the formalism of section 3. All energies are shown as a ratio to the kink energy $E_{\rm k}$ which characterizes the cell-to-cell interaction energy. The parameters were chosen to push the adiabatic limit so that dissipation amounts would be visible on the graph ($E_{\rm k} = 0.19$ eV, $\gamma = 0.0.05$ eV, $f = 100$ GHz, $\tau = 0.35$ fs). The first pair of bars shows the very low dissipation of the shift register, whether it is Landauer-clocked or Bennett-clocked. The second pair of bars shows the dissipation of the Landauer-clocked OR gate (figure 8(b)). When the inputs are 1 and 1 (or 0 and 0) there is no erasure and the energy dissipated is less than $k_B T \ln(2)$. When the inputs differ information is lost and an energy of at least $k_B T \ln(2)$ must be dissipated. In fact the energy dissipated is about $E_{\rm k}$, which needs to be significantly larger than $k_B T \ln(2)$ for the circuits to work reliably in a thermal environment. The third set of bars shows the energy dissipated for the logically reversible circuit formed by combining the OR gate with echoes of the input to the output (figure 8(c)). We see that energy dissipation can indeed be lowered below $k_B T \ln(2)$ by this technique even when, as here, the circuit is Landauer-clocked. The fourth set of data shows the energy dissipated when the OR gate (without

echoes) is simply Bennett-clocked. This is remarkable because the circuit is physically identical to the Landauer-clocked OR gate, but yields vastly less energy dissipation. If the clock speed were substantially slower, the small bars in figure 9 would not be visible at this scale, but the dissipation for the Landauer-clocked OR gate would remain many times larger than $k_B T$.

Figure 9 shows the central results of this work from which several important conclusions can be drawn.

(1) Embedding an irreversible calculation in a reversible circuit by echoing inputs to outputs does indeed result in huge reduction of the power dissipated.
(2) Bennett-clocked QCA circuits can reduce the power dissipated to much less than $k_B T \ln(2)$ without changing circuit complexity. This suggests that QCA may at last provide a practical means of implementing reversible computing.
(3) We verify Landauer's principle by direct time-dependent solutions of the equations of motion for an actual circuit in thermal contact with the environment. The formalism includes the effect of thermal fluctuations from system to environment and from environment to system.
(4) The fact that the shift register dissipates much less than $k_B T \ln(2)$ confirms Landauer's assertion that there is no fundamental lower limit to the energy dissipation cost of *transporting* information [80].

6. Limits to binary logic scaling

Our analysis of molecular QCA provides a useful concrete example in which to examine several recent claims about the physical limits to binary logic scaling. In [75, 76], Zhirnov *et al* make several important claims about fundamental scaling limits. They conclude from a Heisenberg uncertainty principle argument that a binary element cannot be smaller than 1.5 nm. From the requirement that a bit be distinguishable in a thermal environment they argue that an energy equal to the barrier height must be dissipated and that the energy must be at least $k_B T \ln(2)$. They contend that reversible computing requires the complete isolation of the system from the environment, and that any improvement in power dissipation in reversible approaches is illusory because it simply shifts the dissipation to another part of the circuit. Finally, they conclude from this analysis that a successor technology to CMOS must be based on something other than charge. Clearly if their arguments were correct then molecular QCA would be impossible and the results in this paper would have to be in error. Conversely, examining our results in the light of their objections can serve as a specific system in which to assess their claims. We address these issues in turn below.

6.1. Does the uncertainty principle yield a smallest possible bit size?

Zhirnov *et al* proceed from the position-momentum Heisenberg uncertainty relation

$$\Delta x \Delta p \geqslant \hbar. \tag{15}$$

They identify the position uncertainty with the minimum size of a bistable computational element and compute it from $E_{\rm bit}$, the minimum power that must be dissipated when the bit switches:

$$\begin{aligned} X_{\rm min} &= \frac{\hbar}{\Delta p} \\ &= \frac{\hbar}{\sqrt{2 m_e E_{\rm bit}}} \\ &= \frac{\hbar}{\sqrt{2 m_e k_B T \ln(2)}} \\ &= 1.5 \text{ nm } (T = 300 \text{ K}). \end{aligned} \tag{16}$$

Equation (16) is equation (2a) of [75].

The chain of reasoning in equation (16) contains several important flaws. (a) The logic connecting the first line of equation (16) to the second line assumes that $p^2 = 2mE$, but this is true only if the potential $V(x) = 0$. The structure of $V(x)$ is what produces the bistable double-well system and cannot be ignored. One cannot in general simply connect an uncertainty in momentum to an energy. Altering the structure of $V(x)$ changes the relation between the two. (b) Neither is there any reason to associate the energy in (16) with the energy dissipated when the bit is switched. Why is it the dissipated energy and not simply the energy of the bound state? (c) Finally, we have seen that there is no requirement that switching a bit need dissipate $k_B T \ln(2)$; that amount of energy dissipation is required only when a bit is erased. Equation (16) is in fact the answer to the question 'What is an estimate for the width of an infinite square well potential ($V = 0$ inside the well) which would yield a ground-state energy of $k_B T \ln(2)$?'

What *does* limit the physical size of a bit? If the bit is representing information by the position of charge then the potential landscape $V(x)$ determines the two stable configurations and the distance the charge must move between them. Consider a double-well system with a barrier of height V_0 and a distance a between the wells. If the double-well works effectively as a switchable bit for a given value of a, we can achieve the same functionality with a system scaled to a smaller value of a, provided we increase the barrier height, keeping $a^2 V_0$ constant (the usual scaling of the Schrödinger equation). If we could shrink the bit size a to a few thousandths of an angstrom, it would work, and it would function at high temperatures because the energy separations between states would be very large indeed. What limits the physical size of such a bit is our inability to structure a designed potential landscape at that length scale. The only tools we have for fashioning $V(x)$ are atoms and atomic bonds. Since the fundamental constants conspire to make atomic bonds roughly the size of the Bohr radius, we cannot engineer a potential with a smaller length scale. It is not Heisenberg, but Bohr who provides the lower limit.

It is noteworthy that the chemical synthesis of molecular QCA cells has already produced viable bistable bits whose dimensions are smaller than the minimum bit size described by Zhirnov *et al*. The Fehlner molecules [40–43] have charge separation distances of about 0.6 nm. Note also that molecular QCA devices are small in all three spatial dimensions. A 1 nm molecular QCA cell has 1 nm^2 footprint. CMOS at the 6 nm node has a gate length of 6 nm, but the average device area is greater than 0.5 μm^2. Thus the proximity of scaled CMOS to molecular dimensions is not as close as a simple comparison of minimum feature sizes might suggest. (It is also true that differences in architecture make this comparison difficult.)

6.2. Does the need to distinguish a 1 from a 0 in a thermal environment require dissipation of at least $k_BTln(2)$ per bit?

The intuition that the distinguishability criterion, i.e. being able to reliably read and distinguish a 1 from a 0, is connected to energy dissipation is precisely what Landauer refuted. There is no doubt that the barrier to switching when an element is just holding a bit must be larger than k_BT. But there is no reason to equate barrier height with energy dissipated as heat. Neither surmounting a barrier due to thermal excitation, nor tunnelling through a barrier, causes a net transfer of energy from the system to the thermal environment. The key idea of Landauer's adiabatic switching is that the barrier can be lowered, the system switched, and then the barrier raised again.

In the QCA case the distinguishability criterion is helpfully clear. For a QCA shift register, the energy moving from cell to cell as a bit is shifted down the line must indeed be greater than $k_BT\ln(2)$. This energy need not be dissipated at each step, however. Indeed in the Bennett approach it need not be dissipated at all. The signal energy, but not the dissipated energy, must be larger than k_BT for the signal to be robust [22, 23]. Furthermore, the signal energy must be augmented from stage to stage (i.e. there must be true signal power gain) so that the signal does not decay. In QCA, the power gain is provided by the clock. None of this robustness requires a particular amount of energy to be dissipated as heat.

6.3. Does 'reversible computing' require isolation of the system from the thermal environment?

Our theoretical approach, as described in section 3, includes the contact between the system and the environment explicitly. The very notion of energy dissipation, and indeed of temperature, are predicated on considering a system which can exchange energy with its environment. The question is whether there is a fundamental lower limit to how much energy must be transferred to the environment. Landauer's answer (by physical argument) and ours (by direct calculation) is 'no'.

The authors of [76] characterize Landauer in a 1982 paper [81] as affirming that adiabatic operation requires complete isolation from the environment. This is a misreading of Landauer's argument in that paper. He was in [81] contrasting adiabatic reversible computation (low power dissipation), with the more radical notion of 'dissipationless' computing (no power dissipation). Landauer was raising questions about the stability and controllability of systems in which no 'viscosity' at all is present to damp small oscillations. His discussion assumes the correctness of the Landauer principle for adiabatic (non-isolated) reversible systems, and probes what would later become the field of error-correction in quantum computing.

6.4. Are the gains made in power dissipation by 'reversible computing' lost when one considers the system as a whole?

Molecular QCA using buried clocking wires (as in figure 6) provide a helpfully concrete example of where dissipation in such a system can occur. One can distinguish three parts of the system: the active molecular device layer, the clocking wires, and the clocking voltage supply which drives the clocking wires.

We have analysed above the situation in the molecular device layer. Although some dissipation always occurs, there is no fundamental lower limit. At high speeds (>100 GHz) this active layer is still likely to dominate the power dissipation. Moreover, the dissipated power density increases as the device density increases. It is this scaling with device density that is the heart of the problem.

As [76] points out, there is some heat dissipation in the clocking wire circuit, due to the small resistance of the wires themselves, but (*contra* [76]) it can be minimized and is not a fundamental limitation. The wires are driven by a sinusoidal voltage source which smoothly adds charge to raise them up to the appropriate potential, then smoothly removes the charge and lowers the potential. There is never any current through a resistance except the residual resistance of the wires themselves. For a wire network driven with a sinusoidal voltage V at frequency $\omega = 2\pi/T$ with resistance R and capacitance C, the time-averaged power dissipated is simply

$$P = \frac{1}{2}\frac{|V|^2}{R}\left[\frac{(\omega/\omega_0)^2}{(\omega/\omega_0)^2+1}\right] \tag{17}$$

where $\omega_0 \equiv 1/(RC)$. For $\omega \ll \omega_0$ this can be written

$$P = \left[\frac{1}{2}C|V|^2 \quad \frac{2\pi}{T}\right]\left[\frac{\omega}{\omega_0}\right]. \tag{18}$$

The first term in brackets represents the capacitor charging energy per period and the second term is the 'adiabatic reduction factor' which lowers the dissipation due to the gradual nature of the charging and discharging. The power dissipation can be reduced by lowering the residual resistance R ($P \sim R$) or lowering ω ($P \sim \omega^2$).

The authors of [76] unnecessarily complicate the analysis of a simple RC circuit by using a piece-wise-constant voltage source and then worry about maintaining the accuracy of the voltage steps in the presence of thermal noise. The above analysis for a sinusoidal voltage source is simpler and is certainly valid in the presence of thermal noise. Thermal noise does not entail dissipation. Thermal noise involves energy fluctuations that average to zero net energy transfer between system and environment.

The final component of the complete system for molecular QCA is the sinusoidal waveform generator itself. We assume that it may be standard CMOS and can be on or off the molecular electronics chip. It does generate some power dissipation due to the internal resistances of the generator circuit, but this dissipation is unrelated to the 'per device' dissipation that threatens to melt the chip.

6.5. Should charge-based systems be abandoned at the nanoscale?

From an energy viewpoint is there anything special about using charge to represent information? Zhirnov *et al* argue that it important to distinguish between 'charge-based' switching devices and other more exotic devices based on representing information as spin, for example. The fundamental energetics of a bistable system, representing by a double-well energy diagram like figure 1(b), are independent of the particular degrees of freedom used to represent the information. Energy

barriers for a spin system play the same role as for a charge-transfer system. The barrier must be large enough to make different bit states distinguishable in a thermal environment. Switching need not entail dissipating an amount of energy equal to the barrier height. Fundamental energy dissipation considerations do not favour charge-based or spin-based representation information. The conclusion of [75, 76], that only those possible CMOS successor technologies which are based on something other than charge warrant pursuing, is therefore unwarranted.

7. Conclusion

Power dissipation, which has often determined successor electronics technologies in the past, is a crucial consideration for the future of practical computing at molecular length scales. To be successful any technology at that length scale must operate near the fundamental limits of power dissipation per bit computed. A combination of Landauer-clocked and Bennett-clocked molecular QCA, as described here, represents a promising approach to digital logic at this extreme length scale. We have shown, by direct calculation of the equations of motion for actual circuits coupled to the thermal environment, that indeed very low power operation is possible. Our results are not a proof of the correctness of the Landauer–Bennett analysis, but they certainly demonstrate its correctness in this concrete system. The weaknesses of arguments to the contrary are illuminated by examination of a specific system like QCA.

References

[1] Leff H and Rex A 2003 *Maxwell's Demon 2* (Bristol: IOP)
[2] Bennett C H 2003 Notes on Landauer's principle, reversible computation, and maxwell's demon *Stud. Hist. Phil. Mod. Phys.* **34** 501
[3] Bennett C H 1988 Notes on the history of reversible computation *IBM J. Res. Dev.* **32** 16–23
[4] Szilard L 1929 On the decrease of entropy in a thermodynamic system by the intervention of intelligent beings *Z. Phys.* **53** 840–56 (Translation by Rapoport A and Knoller M, reprinted in [1] (pp 110–9, 2nd edition)
[5] Brillouin L 1951 Maxwell's Demon cannot operate: information and entropy. I *J. Appl. Phys.* **22** 334–7
[6] Landauer R 1988 Irreversibility and heat generation in the computing process *IBM J. Res. Dev.* **5** 183–91
[7] Keyes R W and Landauer R 1970 Minimal energy dissipation in logic *IBM J. Res. Dev.* **14** 152–7
[8] Meindl J, Chen Q and Davis J 2001 Limits on silicon nanoelectronics for terascale integration *Science* **293** 2044
[9] Bennett C H 1973 Logical reversibility of computation *IBM J. Res. Dev.* **17** 525–32
[10] Keyes R W 2001 Fundamental limits of silicon technology *Proc. IEEE* **89** 227
[11] Lent C S, Tougaw P D, Porod W and Bernstein G H 1993 Quantum cellular automata *Nanotechnology* **4** 49–57
[12] Lent C S and Tougaw P D 1993 Lines of interacting quantum-dot cells: a binary wire *J. Appl. Phys.* **74** 6227–33
[13] Lent C S, Tougaw P D and Porod W 1993 Bistable saturation in coupled quantum dots for quantum cellular automata *Appl. Phys. Lett.* **62** 714–6
[14] Lent C S and Tougaw P D 1994 Bistable saturation due to single electron charging in rings of tunnel junctions *J. Appl. Phys.* **75** 4077–80
[15] Tougaw P D and Lent C S 1994 Logical devices implemented using quantum cellular automata *J. Appl. Phys.* **75** 1818–25
[16] Lent C S, Tougaw P D and Porod W 1994 Quantum cellular automata: the physics of computing with arrays of quantum dot molecules *Proc. Workshop on Physics and Computation—PhysComp '94* pp 5–13
[17] Tougaw P D and Lent C S 1996 Dynamic behavior of quantum cellular automata *J. Appl. Phys.* **80** 4722–36
[18] Lent C S and Tougaw P D 1997 A device architecture for computing with quantum dots *Proc. IEEE* **85** 541–57
[19] Toth G and Lent C S 1999 Quasiadiabatic switching for metal-island quantum-dot cellular automata *J. Appl. Phys.* **85** 2977–84
[20] Toth G and Lent C S 2001 Role of correlation in the operation of quantum-dot cellular automata *J. Appl. Phys.* **89** 7943–53
[21] Toth G and Lent C S 2001 Quantum computing with quantum-dot cellular automata *Phys. Rev.* A **63** 052315
[22] Timler J and Lent C S 2002 Power gain and dissipation in quantum-dot cellular automata *J. Appl. Phys.* **91** 823–31
[23] Timler J and Lent C S 2003 Maxwell's demon and quantum-dot cellular automata *J. Appl. Phys.* **94** 1050–60
[24] Orlov A O, Amlani I, Bernstein G H, Lent C S and Snider G L 1997 Realization of a functional cell for quantum-dot cellular automata *Science* **277** 928–30
[25] Amlani I, Orlov A O, Snider G L, Lent C S and Bernstein G H 1997 External charge state detection of a double-dot system *Appl. Phys. Lett.* **71** 1730–2
[26] Amlani I, Orlov A O, Snider G L, Lent C S and Bernstein G H 1998 Demonstration of a six-dot quantum cellular automata system *Appl. Phys. Lett.* **72** 2179–81
[27] Amlani I, Orlov A O, Toth G, Lent C S, Bernstein G H and Snider G L 1999 Digital logic gate using quantum-dot cellular automata *Science* **284** 289–91
[28] Orlov A O, Amlani I, Toth G, Lent C S, Bernstein G H and Snider G L 1999 Experimental demonstration of a binary wire for quantum-dot cellular automata *Appl. Phys. Lett.* **74** 2875–7
[29] Amlani I, Orlov A O, Kummamuru R K, Bernstein G H, Lent C S and Snider G L 2000 Experimental demonstration of a leadless quantum-dot cellular automata cell *Appl. Phys. Lett.* **77** 738–40
[30] Orlov A O, Amlani I, Kummamuru R K, Ramasubramaniam R, Toth G, Lent C S, Bernstein G H and Snider G L 2000 Experimental demonstration of clocked single-electron switching in quantum-dot cellular automata *Appl. Phys. Lett.* **77** 295–7
[31] Kummamuru R K, Timler J, Toth G, Lent C S, Ramasubramaniam R, Orlov A O, Bernstein G H and Snider G L 2002 Power gain in a quantum-dot cellular automata latch *Appl. Phys. Lett.* **81** 1332–4
[32] Kummamuru R K, Orlov A O, Lent C S, Bernstein G H and Snider G L 2003 Operation of a quantum-dot cellular (QCA) shift register and analysis of errors *IEEE Trans. Electron Devices* **50** 1906–13
[33] Lent C S 2000 Bypassing the transistor paradigm *Science* **228** 1597–8
[34] Hennessy K and Lent C S 2001 Clocking of molecular quantum-dot cellular automata *J. Vac. Sci. Technol.* B **19** 1752–5
[35] Blair E and Lent C S 2003 An architecture for molecular computing using quantum-dot cellular automata *IEEE-NANO 3rd IEEE Conf. on Nanotechnology* vol 1 (Piscataway, NJ: IEEE) pp 402–5
[36] Lieberman M, Chellamma S, Varughese B, Wang Y L, Lent C S, Bernstein G H, Snider G and Peiris F C 2002 Quantum-dot cellular automata at a molecular scale *Ann. NY Acad. Sci.* **960** 225
[37] Lent C S, Isaksen B and Lieberman M 2003 Molecular quantum-dot cellular automata *J. Am. Chem. Soc.* **125** 1056–63
[38] Lent C S and Isaksen B 2003 Clocked molecular quantum-dot cellular automata *IEEE Trans. Electron Devices* **50** 1890–6

[39] Manimarian M, Snider G L, Lent C S, Sarveswaran V, Lieberman M, Li Z and Fehlner T P 2003 Scanning tunneling microscopy and spectroscopy investigations of QCA molecules *Ultramicroscopy* **97** 55–63

[40] Li Z, Beatty A M and Fehlner T P 2003 Molecular QCA Cells. 1. Structure and functionalization of an unsymmetrical dinuclear mixed-valence complex for surface binding *Inorg. Chem.* **42** 5707–14

[41] Li Z and Fehlner T P 2003 Molecular QCA Cells. 2. Electrochemical characterization of an unsymmetrical dinuclear mixed-valence complex bound to a au surface by an organic linker *Inorg. Chem.* **42** 5715–21

[42] Qi H, Sharma S, Li Z, Snider G L, Orlov A O, Lent C S and Fehlner T P 2003 Molecular QCA cells. Electric field driven switching of a silicon surface bound array of vertically oriented two-dot molecular quantum cellular automata *J. Am. Chem. Soc.* **125** 15250–9

[43] Jiao J, Long G J, Grandjean F, Beatty A M and Fehlner T P 2003 Building blocks for the molecular expression of quantum cellular automata. Isolation and characterization of a covalently bonded square array of two ferrocenium and two ferrocene complexes *J. Am. Chem. Soc.* **125** 7522

[44] Huang J, Tahoori M B and Lombardi F 2004 Defect characterization for scaling of QCA devices *IEEE Symp. on Defect and Fault Tolerant (DFT)*

[45] Fijany A and Toomarian B N 2001 New design for quantum dots cellular automata to obtain fault tolerant logic gates *J. Nanoparticle Res.* **3** 27–37

[46] Walus K, Budiman R A and Jullien G A 2002 Effects of morphological variations of self-assembled nanostructures on quantum-dot cellular automata (QCA) circuits *Frontiers of Integration, An International Workshop on Integrating Nanotechnologies*

[47] Lent C S, Tougaw P D, Brazhnik Y, Weng W W, Porod W, Liu R W and Huang Y F 1996 Quantum cellular neural networks *Superlatt. Microstruct.* **20** 473–8

[48] Gin A, Williams S, Meng H Y and Tougaw P D 1999 Hierarchical design of quantum-dot cellular automata devices *J. Appl. Phys.* **85** 3713–20

[49] Niemier M T and Kogge P M 1999 Logic-in-wire: using quantum dots to implement a microprocessor *ICECS '99: Int. Conf. on Electronics, Circuits, and Systems*

[50] Pasky J R, Henry L and Tougaw P D 2000 Regular arrays of quantum-dot cellular automata macrocells *J. Appl. Phys.* **87** 8604–9

[51] Csurgay A I, Porod W and Lent C S 2000 Signal processing with near-neighbor-coupled time-varying quantum-dot arrays *IEEE Trans. Circuits Syst.* I **47** 1212–23

[52] Niemier M T and Kogge P M 2001 Problems in designing with QCAs: layout = timing *Int. J. Circuit Theor. Appl.* **29** 49–62

[53] Cardenas-Barrera J L, Platoniotis K N and Venetsanopoulos A N 2002 QCA implementation of a multichannel filter for image processing *Math. Prob. Eng.* **8** 87–99

[54] Frost S E, Rodrigues A F, Janiszewski A W, Rausch R T and Kogge P M 2002 Memory in motion: a study of storage structures in QCA *1st Workshop on Non-Silicon Computation*

[55] Niemier M T, Rodrigues A F and Kogge P M 2002 A potentially implementable FPGA for quantum dot cellular automata *1st Workshop on Non-Silicon Computation*

[56] Armstrong C D and Humphreys W M 2003 The development of design tools for fault tolerant quantum dot cellular automata based logic *2nd Int. Workshop on Quantum Dots for Quantum Computing and Classical Size Effect Circuits*

[57] Tahoori M B, Huang J, Momenzadeh M and Lombardi F 2004 Testing quantum cellular automata *IEEE Transaction on Nanotechnology (TNANO)*

[58] Dimitrov V S, Jullien G A and Walus K 2002 Quantum-dot cellular automata carry-look-ahead adder and barrel shifter *IEEE Emerging Telecommunications Technologies Conf.*

[59] Walus K, Vetteth A, Jullien G A and Dimitrov V S 2003 RAM design using quantum-dot cellular automata *NanoTechnology Conf.* vol 2, pp 160–3

[60] Walus K 2006 QCADesigner Home Page, http://www.qcadesigner.ca

[61] Single C, Augke R, Prins E E, Wharam D A and Kern D P 2000 Towards quantum cellular automata operation in silicon: transport properties of silicon multiple dot structures *Superlatt. Microstruct.* **28** 429–34

[62] Single C, Rugke A and Prins E E 2001 Simultaneous operation of two adjacent double dots in silicon *Appl. Phys. Lett.* **78** 1421–3

[63] Cowburn R P and Welland M E 2000 Room temperature magnetic quantum cellular automata *Science* **287** 1466–8

[64] Csaba G and Porod W 2002 Simulation of field coupled computing architectures based on magnetic dot arrays *J. Comp. Elect.* **1** 87–91

[65] Imre A, Zhou L, Orlov A, Csaba G, Bernstein G H, Porod W and Metlushko V 2004 Application of mesoscopic magnetic rings for logic devices *4th IEEE Conf. on Nanotechnology* pp 137–9

[66] Brum J A and Hawrylak P 1997 Coupled quantum dots as quantum exclusive-OR gate *Superlatt. Microstruct.* **22** 431

[67] Openov L A and Bychkov A M 1998 Non-dissipative logic device NOT based on two coupled quantum dots *Phys. Low-Dim. Struct.* **9/10** 153 (*Preprint* cond-mat/9809112)

[68] Sanders G D, Kim K W and Holton W C 1999 Optically driven quantum-dot quantum computer *Phys. Rev.* B **60** 4146

[69] Balandin A and Wang K L 1999 Feasibility study of the quantum XOR gate based on coupled asymmetric semiconductor quantum dots *Superlatt. Microstruct.* **25** 509

[70] Openov L A 1999 Resonant electron transfer between quantum dots *Phys. Rev.* B **60** 8798

[71] Fedichkin L, Yanchenko M and Valiev K A 2000 Coherent charge qubits based on GaAs quantum dots with a built-in barrier *Nanotechnology* **11** 387

[72] Biolatti E, Iotti R C, Zanardi P and Rossi F 2000 Quantum information processing with semiconductor macroatoms *Phys. Rev. Lett.* **85** 5647

[73] Gaudreau L, Studenikin S, Sachrajda A, Zawadzki P, Kam A, Lapointe J, Korkusinski M and Hawrylak P 2006 The stability diagram of a few electron artificial triatom *Preprint* cond-mat/0601597

[74] Fujisawa T *et al* 2006 Time-dependent single-electron transport through quantum dots *Rep. Prog. Phys.* **69** 759–96

[75] Zhirnov V V, Cavin R K, Hutchby J A and Bourianoff G I 2003 Limits to binary logic switch scaling—a gedanken model *Proc. IEEE* **91** 1934

[76] Cavin R K, Zhirnov V V, Hutchby J A and Bourianoff G I 2005 Energy barriers, demons, and minimum energy operation of electronic devices *Noise in Devices and Circuits III* (*Proc. SPIE* vol 5844) ed A Balandin, F Danneville, M J Deen and D M Fleetwood (Bellingham, WA: SPIE) pp 1–9

[77] Frisch M J *et al* 2004 *Gaussian 03, Revision C.02* (Wallingford, CT: Gaussian)

[78] Mahler G and Weberrub V A 1995 *Quantum Networks: Dynamics of Open Nanostructures* (New York: Springer)

[79] Martini I B, Ma B, Ros T D, Helgeson R, Wudl F and Schwartz B J 2000 Ultrafast competition between energy and charge transfer in a functionalized electron donor fullerene derivative *Chem. Phys. Lett.* **327** 253–62

[80] Landauer R 1987 Energy requirements in communication *Appl. Phys. Lett.* **51** 2056–8

[81] Landauer R 1982 Uncertainty principle and minimal energy dissipation in the computer *Int. J. Theor. Phys.* **21** 283